AMER. ZOOL., 40:101–122 (2000)

Function of the Caudal Fin During Locomotion in Fishes: Kinematics, Flow Visualization, and Evolutionary Patterns[1]

GEORGE V. LAUDER[2]

Department of Ecology and Evolutionary Biology, University of California, Irvine, California 92697

SYNOPSIS. One of the most prominent characteristics of early vertebrates is the elongate caudal fin bearing fin rays. The caudal fin represents a fundamental design feature of vertebrates that predates the origin of jaws and is found in both agnathans and gnathostomes. The caudal fin also represents the most posterior region of the vertebrate axis and is the location where fluid, accelerated by movement of the body anteriorly, is shed into the surrounding medium. Despite the extensive fossil record of the caudal fin, the use of caudal characters for systematic studies, and the importance of tail function for understanding locomotor dynamics in fishes, few experimental studies have been undertaken of caudal fin function. In this paper I review two experimental approaches which promise to provide new insights into the function and evolution of the caudal fin: three-dimensional kinematic analysis, and quantitative flow measurements in the wake of freely-swimming fishes using digital particle image velocimetry (DPIV). These methods are then applied to the function of the caudal fin during steady swimming in fishes with heterocercal and homocercal morphologies: chondrichthyians (leopard sharks) and ray-fined fishes (sturgeon and bluegill sunfish). The caudal fin of leopard sharks functions in a manner consistent with the classical model of heterocercal tail function in which the caudal surface moves at an acute angle to the horizontal plane, and hence is expected to generate lift forces and torques which must be counteracted anteriorly by the body and pectoral fins. An alternative model in which the shark tail produces a reactive force that acts through the center of mass is not supported. The sturgeon heterocercal tail is extremely flexible and the upper tail lobe trails the lower during the fin beat cycle. The sturgeon tail does not function according to the classical model of the heterocercal tail, and is hypothesized to generate reactive forces oriented near the center of mass of the body which is tilted at an angle to the flow during steady locomotion. Functional analysis of the homocercal tail of bluegill shows that the dorsal and ventral lobes do not function symmetrically as expected. Rather, the dorsal lobe undergoes greater lateral excursions and moves at higher velocities than the ventral lobe. The surface of the dorsal lobe also achieves a significantly acute angle to the horizontal plane suggesting that the homocercal tail of bluegill generates lift during steady swimming. These movements are actively generated by the hypochordal longitudinalis muscle within the tail. This result, combined with DPIV flow visualization data, suggest a new hypothesis for the function of the homocercal tail: the homocercal tail generates tilted and linked vortex rings with a central jet inclined posteroventrally, producing an anterodorsal reactive force on the body which generates lift and torque in the manner expected of a heterocercal tail. These results show that the application of new techniques to the study of caudal fin function in fishes reveals a previously unknown diversity of homocercal and heterocercal tail function, and that morphological characterizations of caudal fins do not accurately reflect *in vivo* function.

[1] From the Symposium on *The Function and Evolution of the Vertebrate Axis* presented at the Annual Meeting of the Society of Integrative and Comparative Biology, 6–10 January 1999, at Denver, Colorado.

[2] Present address of George V. Lauder is: Museum of Comparative Zoology, Harvard University, 26 Oxford St., Cambridge, MA 02138, E-mail: GLauder@oeb.harvard.edu

INTRODUCTION

One of the most prominent characteristics of early vertebrate fossils is the elongate tail bearing fin rays (Fig. 1). This basic structure of the caudal fin represents a fundamental design feature of vertebrates that predates the origin of jaws and is found in both agnathans and gnathostomes. Early vertebrates show a considerable diversity of tail shapes, ranging from the forked-tail of agnathan 'thelodonts' (Wilson and Caldwell, 1993, [Fig. 1A]), to the better known caudal morphologies in ostracoderms (Fig. 1B–D). Elasmobranchs (sharks) and ray-finned fishes also show considerable diversity in caudal fin morphology, and diversification in structures involved in locomotion has been a major theme in the evolution of these clades (Lauder, 1989). Because of the prominence of the caudal fin in early vertebrate fossils, its importance in locomotion, and the diversity of tail shapes, nearly all textbooks of vertebrate paleontology, anatomy, and ichthyology discuss the evolution of the tail. For example, Romer (1966, p. 5) includes a discussion of caudal fin structure in his introductory chapter on basic vertebrate features, and similar analyses can be found in Hildebrand (1974), Carroll (1988), Pough *et al.* (1989), Kardong (1994), and Helfman *et al.*, (1997). The design of the caudal fin of fishes has also attracted attention from workers interested in the mechanics and hydrodynamics of locomotion in fishes (Bainbridge, 1963; Alexander, 1965; Lighthill, 1969; Videler, 1975; DuBois *et al.*, 1976; Thomson, 1976). The caudal fin represents the distal region of the vertebrate axis and is the region of the body where fluid accelerated anteriorly is shed into the surrounding medium. As such, the morphology of the caudal fin may influence the forces exerted on the fluid by a swimming fish and in turn the reaction forces experienced by the body during locomotion.

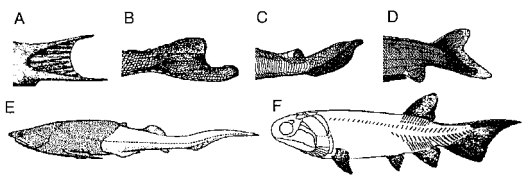

FIG. 1. Upper row: diagram of fish tails to show different configurations in agnathans (A–D). Lower row: tail shape in a primitive gnathostome E. the arthrodire (*Arctolepis*) and a primitive ray-finned fish F. (*Carboveles*). The heterocercal tail configuration shown in F is plesiomorphic for ray-finned fishes. Modified from Wilson and Caldwell (1993), Carroll (1988), and Romer (1966).

However, compared to the extensive analyses of myotomal muscle function that have been conducted over the last two decades (e.g., Bone *et al.*, 1978; Johnsrude and Webb, 1985; Rome *et al.*, 1988, 1993; Johnston, 1991; Jayne and Lauder, 1994b, 1995; Shadwick *et al.*, 1998) and studies of axial musculoskeletal structure and function (Symmons, 1979; Hebrank, 1982; Long, 1992, 1995; Westneat *et al.*, 1993; Jayne and Lauder, 1994a), comparatively little is known about how the tail of fishes functions during swimming. Indeed, we lack even basic kinematic data on the movement of the caudal fin during steady swimming, and have even less information on the effect of different tail shapes on patterns of fluid flow and thrust production.

FUNCTIONAL AND PHYLOGENETIC PERSPECTIVE

The diversity of caudal structure in fishes has been grouped into broad categories based primarily on the shape and relative sizes of the upper and lower tail lobes and the position of the vertebral column within the tail. The basic classification of fin shape dates from Louis Agassiz in 1833 who proposed the terms ''heterocercal'' (for externally asymmetrical tails with larger dorsal lobes containing the terminal extension of the vertebral column or notochord) and ''homocercal'' (for tails which are externally symmetrical and have equal-sized upper and lower lobes). In homocercal tails, the vertebral column typically terminates near the base of the skeletal elements supporting the tail (hypural bones in teleosts), and although the internal caudal skeleton is not completely dorsoventrally symmetrical, the dorsal and ventral lobes of the tail are nearly equivalent in area and composition.

The heterocercal caudal fin is found in a

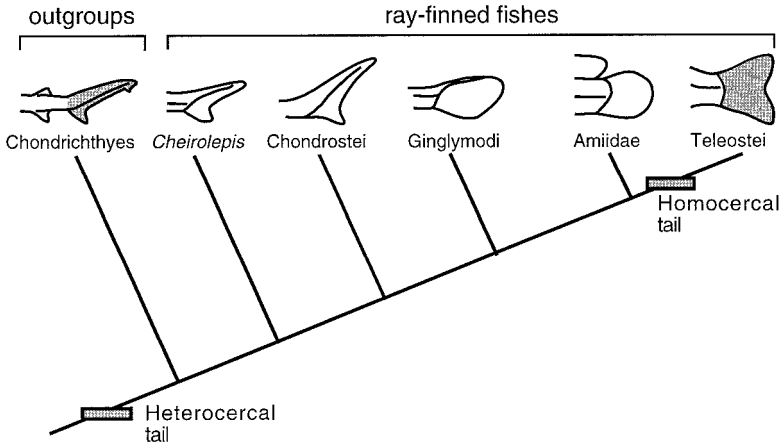

FIG. 2. Highly simplified phylogeny of ray-finned fishes with a chondrichthyian outgroup clade to show the major pattern of caudal fin evolution from the primitive heterocercal condition to the derived homocercal configuration. Numerous different tail configurations (not shown in this figure) exist within the ray-finned fishes, even among basal clades (see *e.g.*, Moy-Thomas and Miles, 1971).

diversity of fish clades and is believed to be primitive for sharks and ray-finned fishes (Figs. 1E, F, 2) despite considerable diversity in the morphology of tail shapes in fossil fishes (see Moy-Thomas and Miles, 1971). The homocercal tail represents a derived morphology (Fig. 2) that is found within all major clades of ray-finned fishes. Although additional terms are used to describe variants of these two shapes, Agassiz's terminology is retained in all modern textbooks. Broad evolutionary patterns of caudal fin structure have now been relatively well documented in fishes, and the internal anatomy of the caudal fin is a common source of characters for phylogenetic analysis (Patterson, 1968, 1973; Schultze and Arratia, 1986, 1988; Arratia, 1991).

The current literature contains several hypotheses about the function of caudal fins of different shape, and much of this discussion has focused on the difference between heterocercal and homocercal tails (Alexander, 1965; Aleev, 1969; Magnuson, 1970; Thomson, 1971, 1976; Hopson, 1974; Thomson and Simanek, 1977; Webb and Smith, 1980). Because the vertebral column or notochord extends into the dorsal lobe of the tail in fishes with heterocercal caudal fins, this dorsal lobe has classically been believed to be stiffer and hence to lead the ventral lobe as it moves laterally during the tail beat (Fig. 3). Fin rays that comprise the ventral lobe are relatively flexible and follow the leading dorsal edge of the tail. Carter (1967, pp. 111–112) has succinctly summarized the classical view of heterocercal tail function by noting that "the ventral lobe of the tail, being more flexible than the dorsal lobe, which contains the vertebral column, lags behind as the tail swings from side to side and passes through the water at an angle to the vertical." Motion of the tail at an angle to the vertical (Fig. 3) gives rise to lift forces perpendicular to the horizontal and torque about the center of mass that tend to pitch the head of the fish ventrally. Such torques are proposed to be counteracted anteriorly by lift forces generated by the head and pectoral fins.

Thomson (1976) proposed a different view of heterocercal tail function based on his observation that the ventral lobe of the tail appeared to lead the dorsal lobe in films taken behind the tail during locomotion by sharks in aquaria. Under this model, the reaction force generated by movement of the heterocercal tail was proposed to be directed anteroventrally through the center of mass of the body (Fig. 3). The classical model and that proposed by Thomson make fundamentally different predictions about expected patterns of heterocercal tail move-

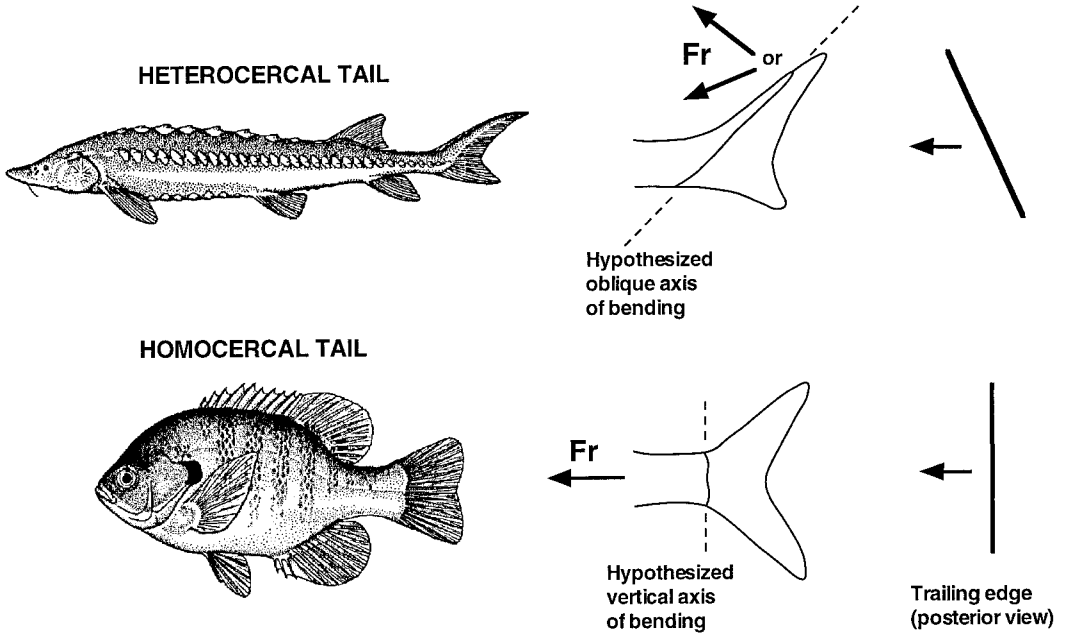

FIG. 3. Diagram of two extant ray-finned fishes, a sturgeon, *Acipenser*, (above) and a bluegill, *Lepomis*, (below) to illustrate heterocercal and homocercal tail shapes, respectively. The middle panel shows literature interpretations of caudal fin function (in lateral view) with the hypothesized axis of bending and direction of thrust (Affleck, 1950). Two alternative thrust directions are shown for the heterocercal tail; one based on the classical model of heterocercal tail lift (upper arrow), and the other on the model of Thomson (1976, lower arrow), in which thrust is directed toward the center of mass of the fish. The right panel shows the caudal fin as a single line in posterior view as it would appear under the classical hypotheses of heterocercal and homocercal tail function. Fr: reactive force on the fish resulting from forces generated on the water during the tail beat. Fish pictures courtesy of S. M. McGinnis (1984, *Freshwater Fishes of California.*© The Regents of the University of California.)

ment and about the effect of tail motion on the water leaving the trailing edge.

The homocercal tail, in contrast, has been nearly universally held to generate a reaction force directed forward (near the center of mass) because of the vertical axis of bending and to move symmetrically with both dorsal and ventral lobes moving in synchrony (Fig. 3) (Affleck, 1950; Patterson, 1968; Gosline, 1971). Some authors have noted more complex actions of homocercal caudal fins than simple symmetrical dorsal and ventral lobe motion (Bainbridge, 1963; Fierstine and Walters, 1968; Aleev, 1969; Videler, 1975), but no study to date has quantified motion of the homocercal caudal fin to examine explicitly the classical view of symmetrical function during steady horizontal locomotion.

This paper has three aims. First, I will discuss two experimental approaches to the study of caudal fin function in fishes that are likely to greatly enhance our ability to quantify relevant functional attributes of fish fins. Second, I show data resulting from the application of these methods to analyses of heterocercal and homocercal tail morphologies during steady swimming in chondrichthyians (leopard sharks) and ray-fined fishes (sturgeon and bluegill sunfish). Third, based on these experimental data, I reevaluate the classical models of homocercal and heterocercal tail function.

TECHNIQUES FOR ANALYZING CAUDAL FIN FUNCTION

Two attributes of fin function in fishes that have received the least attention are (1) a precise description of the motion of surface elements of the fin and (2) an analysis of the effect that fin motions have on the water. Since the presence of fins as control

surfaces in fishes is a prominent aspect of their biological design, it is at first glance surprising that so little is known about how fins move and what effect such movements have on fluid motion. But measuring both fin and fluid motion accurately and in a time-dependent manner is a difficult proposition. Fish fins are thin and often diaphanous and monochromatic, making identification of specific points difficult, while quantifying motion of a clear fluid is a difficult problem of long-standing (Nakayama, 1988; Yang, 1989; Nieuwstadt, 1993; Moin and Kim, 1997). Fortunately, recent developments in experimental methodology have allowed the application of video and fluid dynamics techniques to the study of fin and fluid movement, and we are now in a position to generate new data on the function of fins.

Three-dimensional kinematics

Given that the vast majority of research on fish locomotion has involved analysis of body deformation and myotomal muscle function, it is perhaps not surprising that the most common images in the literature of fishes swimming are ventral or dorsal views. Such images are usually obtained by aiming a video camera at a mirror mounted either above or below the swimming fish, and quantifying deformation of the body by digitizing either the midline or the silhouette. But examination of the shape of the tail in these images reveals that changes in thickness occur which indicate that there are as yet unrecognized alterations in caudal fin shape that are not well revealed by ventral or dorsal views (*e.g.*, Gray, 1933, 1968; Aleev, 1969). This suggests that a three-dimensional analysis is needed to capture the complex motions of fins.

A three-dimensional analysis would also alleviate the possibility of serious error when a two-dimensional analysis alone is used. One way in which such errors can arise is shown in Figure 4 which depicts a three-dimensional space defined by X, Y, and Z axes. Such a space may represent the working section of a flow tank, or the aquarium within which an experiment is conducted. The XZ plane represents the horizontal or frontal plane, the XY plane the vertical or parasaggital plane, and the YZ plane the transverse section. If a triangle is suspended within this space to represent the tail of a fish swimming in a flow tank, then water would flow through the YZ plane parallel to the XY plane. The video images obtained through the XY plane would represent a lateral view while images through the YZ plane a posterior view. By examining the projection of the triangle on the XZ plane and the locations of the vertices on the Z axis, it is possible to see that this triangle has been positioned so that it forms an acute angle to the XZ plane; that is, it is inclined toward increasing Z values and vertex three leads the triangle as it moves toward the XY plane. Water influenced by motion of the tail in this way would be expected to move ventrally, so directed by the ventrally inclined surface of the triangle. However, if we rely on a posterior view alone, projection of the trailing edge (line segment 2-1) onto the YZ plane is inclined dorsally suggesting, erroneously, that fluid influenced by such a motion might be directed dorsally. Reliance on a lateral or ventral view alone provides similarly misleading information on motion in the other planes. Lauder and Jayne (1996) showed that angles of fin surfaces estimated from two-dimensional analyses can be in error by as much as 83° from the correct three-dimensional angle (and further details about 3D angle calculations can be found in that paper).

In order to record three-dimensional data on caudal fin movements during steady locomotion, I have used the experimental design illustrated in Figure 5. Two synchronized video cameras record orthogonal planar views of the fins at 250 images per second. One camera images a lateral (XY view) through the side of the flow tank while the second camera is aimed at a small mirror located in the flow posterior to the swimming fish. By aligning this mirror at a 45° angle to the flow, the camera images the posterior (YZ view) of the fins. Information from both cameras together provides X, Y, and Z coordinates for points on the fins. In order to facilitate repeated and accurate recognition of specific locations on the fin, fish are anesthetized prior to each

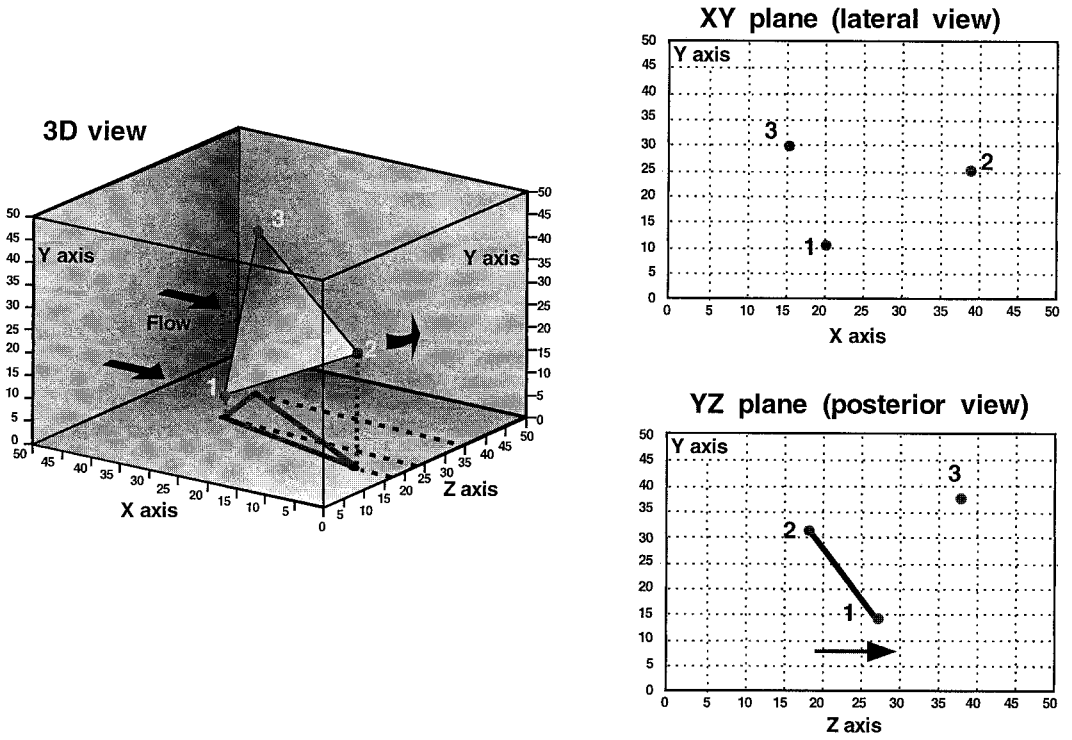

FIG. 4. One source of error in two-dimensional kinematic analyses. Left panel: three-dimensional representation of a triangle oriented in space so that the ventral surface is inclined at an acute angle to the XZ plane. Note the projection of the triangle onto the XZ plane and the relative positions of the vertices on the Z-axis. A tail surface element oriented in such a position and moving toward the XY plane (into the page, or toward increasingly large Z-axis values) would be expected to push water posteroventrally. Given this orientation, the position of the three points in a two-dimensional view is shown on the right. The upper panel shows the XY position of the three vertices, and the lower panel the position of the vertices in the YZ plane. Note that even though the orientation of the triangle in three-dimensions is at an acute angle to the XZ plane, the two-dimensional projection of the line segment 1–2 appears to be inclined upward, *opposite* to the true orientation of the triangle.

experiment and small markers are glued bilaterally onto the fin. In the image shown in Figure 5, a triangular marker arrangement has been used on both the dorsal and ventral lobes of the tail. Such triangular patterns allow reconstruction of the *surface* orientation of fin regions through calculation of planar angles of intersection between triangular fin elements and the three reference planes (Lauder and Jayne, 1996).

Location of the posterior-view mirror at least one to two body lengths posterior to the trailing edge of the tail and against the downstream flow grid (which restricts recirculatory vortices downstream from the mirror and hence their impact on flow immediately upstream from the mirror) minimizes any disturbance of the flow caused by the mirror in the region of the swimming fish. Analyses of variance conducted for leopard sharks swimming in this apparatus (Ferry and Lauder, 1996) and similar analyses for bluegill showed that the presence of the mirror in the flow had no significant effect on either tail beat amplitude or frequency ($P > 0.27$), suggesting that the mirror has little impact on the kinematics of the tail beat.

Digital particle image velocimetry (DPIV)

While quantifying the three-dimensional motion of the caudal fin is one critical component of understanding caudal fin function, it is also necessary to evaluate the impact that movement of the fin has on the fluid. By understanding the fluid motion in-

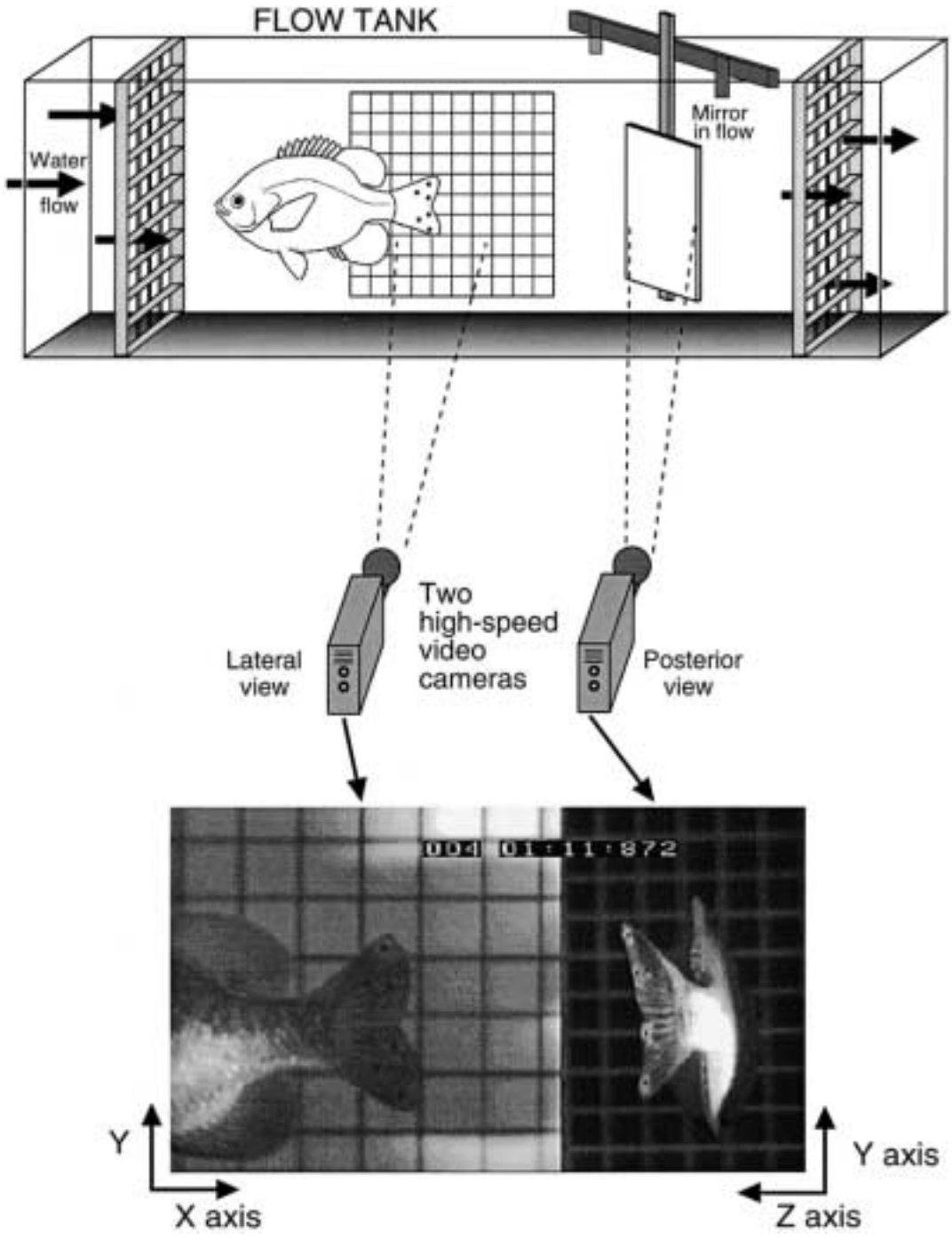

FIG. 5. Schematic view of flow tank, mirror and video camera arrangement used to obtain three-dimensional data from swimming fish. One camera is aimed at the lateral tail surface and provides data in the XY plane, while a second, synchronized, camera is aimed at a small mirror placed in the flow downstream from the swimming fish. This second camera provides a posterior (YZ) view of tail function. Markers placed on the tail (three are shown on both the upper and lower lobes) allow precise identification of specific points on the tail in three dimensions. The video image below shows a sample image obtained from a bluegill sunfish (*Lepomis macrochirus*) swimming at 1.2 lengths/sec.

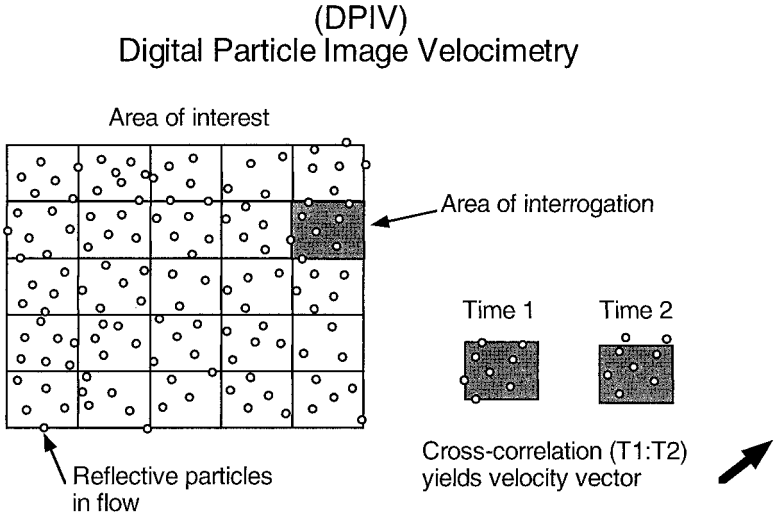

FIG. 6. Schematic representation of the DPIV (digital particle image velocimetry) technique for the study of fluid flow. Small reflective particles are placed in the water and light from a laser is focused into a light sheet which reflects off of individual particles and is imaged by high-speed video. The area of interest in the wake of a swimming fish is divided into discrete areas of interrogation (a 5 by 5 matrix giving 25 such areas is shown here). A two-dimensional cross-correlation analysis of images separated in time by Δt (4 ms at a filming rate of 250 fps) provides an estimate of the fluid velocity in each area yielding a total of 25 velocity vectors at this time. Additional analyses at later times generate an analysis of time-dependent flow patterns. Further description is provided in the text.

duced by action of the caudal fin, the forces exerted on the fluid and the direction of those forces can be estimated. While analyses of locomotion on land have traditionally used force plates to quantify the forces exerted by limbs during locomotion (Cavagna, 1975; Biewener and Full, 1992), a technique allowing similar measurements has not been available until recently for the aquatic realm.

The technique of DPIV (digital particle image velocimetry) provides a means of quantifying fluid flow and of calculating forces exerted by fishes swimming *in vivo*. By visualizing flow in two or more dimensions, vortices formed by fin movement can be reconstructed and the orthogonal components of momentum and force calculated (*e.g.*, Lauder *et al.*, 1996; Drucker and Lauder, 1999; Wolfgang *et al.*, 1999; Wilga and Lauder, 1999). Such measurements allow a direct test of functional hypotheses.

Figure 6 illustrates the basic principle of DPIV as used in our experiments visualizing flow in the wake of the caudal fin. Water in a flow tank is seeded with small (12 μ mean diameter) silver coated glass beads which reflect light from an argon-ion laser. The laser beam is focused via a series of lenses into a light sheet approximately 10 cm wide and 1–2 mm thick. The experimental arrangement is as shown in Figure 5 with the addition of a laser and light sheet extending into the flow tank. Movement of the optical components allows the laser light sheet to be oriented into three orthogonal planes (video cameras are also appropriately repositioned to provide an image of the light sheet), and video images are taken of the light reflected from the particles in the flow (also see Drucker and Lauder, 1999). The particles are carried through the light sheet with water movement, and as the flow is disturbed by movement of the tail particles move with the flow and their reflections are captured on video. By using two simultaneous video cameras, one camera can capture the particle reflections while the other images the position of the fish relative to the light sheet. This allows determination of precisely which portion of the tail is acting on the fluid. By repositioning the fish in the flow tank, images of the flow

around different regions of the tail can be obtained.

Analysis proceeds by choosing pairs of video images (separated in time by 4 ms) that capture flow in the wake behind the tail. The area of interest in the wake (typically a 10 cm^2 region, see Fig. 6) is then selected and divided into a matrix of discrete smaller areas of interrogation. For the analyses presented here, a 20*20 matrix of areas of interrogation was used. A standard two-dimensional cross-correlation analysis is then used to compare the pixel intensities at one time to that Δt later, and each cross-correlation analysis yields a velocity vector that estimates the direction and speed of flow in that area of interrogation (Raffel *et al.*, 1998). Given a 20*20 matrix of areas, a regularly spaced array of 400 velocity vectors is obtained that provides a quantitative estimate of flow in the light sheet at that time. From this matrix of velocity vectors, fluid vorticity, momentum, circulation, and force can be calculated (Drucker and Lauder, 1999) using standard methods (Rayner, 1979; Spedding *et al.*, 1984; Spedding and Maxworthy, 1986; Spedding, 1987).

FUNCTION OF THE CAUDAL FIN DURING LOCOMOTION IN ELASMOBRANCHS

As noted above, there are two alternative views of heterocercal tail function in sharks, and three-dimensional kinematic data are needed to distinguish between the two models. By swimming leopard sharks, *Triakis semifasciata*, in a flow tank with the dual camera arrangement shown in Figure 5, Ferry and Lauder (1996) were able to quantify the movement of specific points on the heterocercal tail in three-dimensions and to calculate the three-dimensional orientation of seven triangular fin elements. The classical model predicts that the XZ angle of tail triangles should be greater than 90° as the tail moves toward increasing Z values indicating that the triangular surfaces are oriented in a manner predicted to force water posteroventrally and hence creating a reactive lift force on the tail (Fig. 3). In contrast, the alternative model predicts that the XZ angle will be less than 90° with the expectation that water influenced by motion of the tail will be directed posterodorsally and thus create a reaction force directed slightly ventrally through the center of mass.

Representative data from two tail triangles are plotted in Figure 7 along with data showing the lateral (Z) excursion of two points on the tail. For most of the tail beat, the XZ angles are greater than 90° supporting the classical model of heterocercal tail function. Ferry and Lauder (1996) presented additional evidence in support of this model in the form of dye injection near the tail which showed that the leopard shark tail directs water in a posteroventral direction, consistent with the classical model.

The model proposed by Thomson (1976) for heterocercal tail function resulted in part from film images of shark tails taken in posterior view as sharks swam in large aquaria. Such views appear to show that the ventral lobe of the tail leads the dorsal for portions of the tail beat and that the tail appears to be oriented in a manner that might direct a reactive force ventrally through the center of mass. However, the three-dimensional angles calculated for leopard shark tails show that despite appearances, the tail surfaces are oriented in a manner consistent with the classical hypothesis. In addition, it is possible that the posterior views that formed the initial evidence for an alternative to the classical model were subject to the difficulties diagrammed in Figure 4: if only a posterior view is available, a surface may appear to be in a substantially different orientation from its actual three-dimensional position.

FUNCTION OF THE CAUDAL FIN DURING LOCOMOTION IN STURGEON

In order to test the generality of the conclusions described above for heterocercal tails in taxa other than sharks, I examined the kinematics and fluid flow patterns around the tail of swimming sturgeon *Acipenser transmontanus*. Sturgeon are members of a basal clade of ray-finned fishes (Grande and Bemis, 1996; Bemis *et al.*, 1997) and possess heterocercal tails (Fig. 3): the vertebral column extends into the dorsal lobe while the ventral lobe is composed of fin rays.

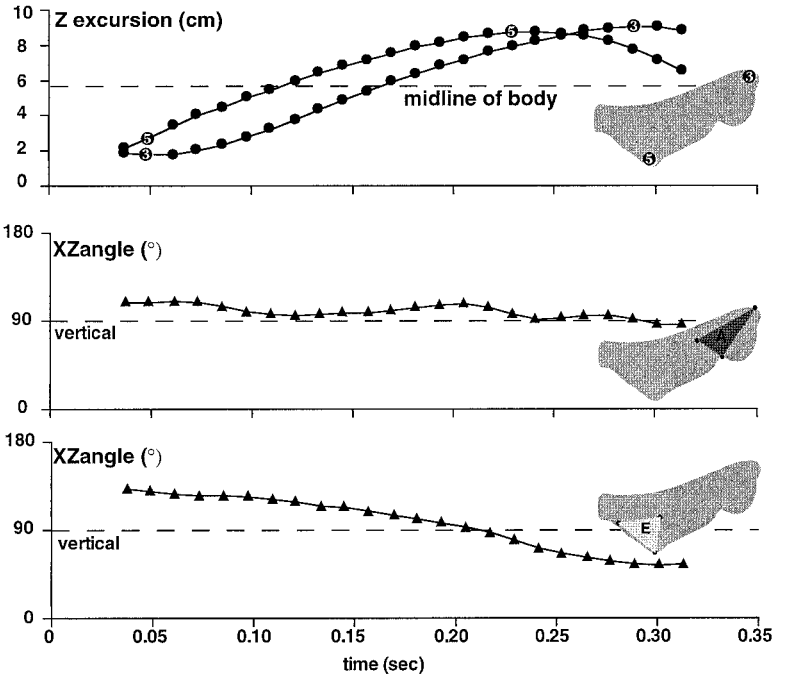

FIG. 7. Heterocercal tail kinematics in the leopard shark, *Triakis semifasciata* swimming steadily at 1.2 lengths/sec. Z-dimension excursions (upper panel) of two points on the tail and the three-dimensional angles of two tail triangles with the XZ plane. Note that for most of the tail beat, the orientation of these two triangular elements is greater than 90° indicating that the tail is moving in accordance with the classical model of heterocercal tail function.

Kinematic analysis was accomplished by swimming sturgeon at 1.2 lengths/sec in a flow tank as illustrated in Figure 5. Prior to swimming fish in the flow tank, individuals were anesthetized and small white markers attached to the tail in order to provide reliable and repeatable locations for digitizing. The tail surface was divided into six triangular elements and the orientations of these elements in three-dimensions was calculated.

Figure 8 shows six representative video frames, each illustrating a simultaneous lateral and posterior view of the tail. It is apparent from the first frame that the dorsal lobe containing the vertebral column does *not* lead the tail beat. Rather, the dorsal lobe trails the central region of the tail and as the central and ventral tail areas reach their maximum left lateral excursion and begin to move back toward the right side, the dorsal tail region is still moving to the left. The arrows in Figure 8 show the direction of dorsal and ventral tail movement, and it is clear that for much of the tail beat the dorsal and ventral lobes of the tail are moving in opposite directions. This is a very different movement pattern than seen for the leopard shark tail. The sturgeon tail behaves mechanically as an extremely flexible sheet with flexible dorsal and ventral lobes following the central tail region.

Graphs of three-dimensional orientations of sturgeon tail triangles (Fig. 9) show that the XZ angles oscillate about a mean angle of 90° during the tail beat indicating that these triangles do not maintain a consistent acute orientation relative to the horizontal plane as does the leopard shark tail. By calculating a ''scaled movement vector'' for each triangle on the sturgeon tail following the procedure described for sharks in Ferry and Lauder (1996) and then summing these vectors over the entire tail, the oscillation of Y-dimensional orientation of the tail can be seen (Fig. 10). Scaled movement vectors

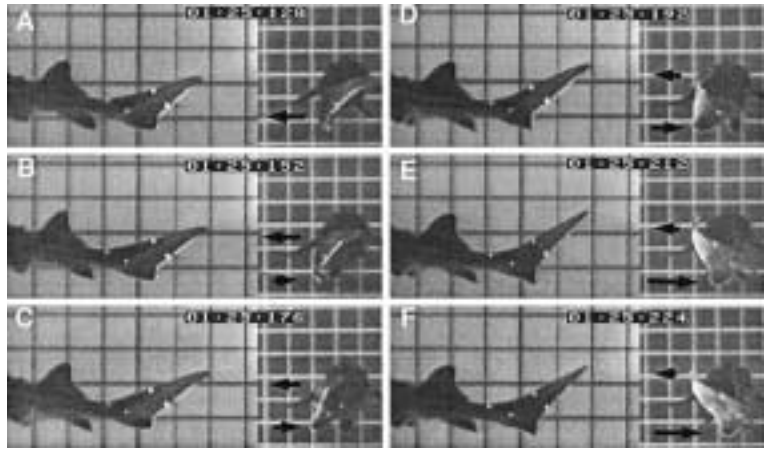

FIG. 8. Video images of caudal fin function in the sturgeon, *Acipenser transmontanus* swimming steadily at 1.2 lengths/sec. Each video frame is split into a lateral portion on the left and a posterior view on the right and resulted from the experimental arrangement illustrated in Figure 5. The grid seen in the posterior view is the upstream baffle in the flow tank. The time of each frame (in ms) is given by the last three digits of the time code at the top of each panel. The monochromatic sturgeon tail has been bilaterally marked with small white markers at four locations to facilitate digitizing three dimensional coordinates of tail elements. Arrows indicate relative movement of the upper and lower portions of the tail, and the length of the arrow is roughly proportional to the velocity of the respective tail element. In frame A, the whole tail is momentarily moving to the left as a unit, but for most of the tail beat, the dorsal and ventral tail lobes move in opposite directions, and the upper lobe trails behind the lower.

reflect both the area of tail and the velocity of the triangle centroids resolved into X, Y, and Z components. The X movement vectors are consistently positive and the Z vectors oscillate negative and then positive as the tail beats from side to side. These X and Z component patterns are similar to those seen for sharks as expected given oscillatory tail movement and the necessity for thrust production. However, the Y component displays a different pattern than seen for sharks, oscillating about a horizontal orientation, whereas in the leopard shark Y movement vectors are consistently negative.

Measurement of fluid motion in the wake of the tail of a swimming sturgeon (Liao and Lauder, 2000) reveals two counter-rotating centers of vorticity (in the XY plane) which reflect a section through a vortex ring shed by the beating tail. Production of vortex rings during locomotion has been predicted on the basis of theory; vorticity arises as water moves around the trailing edge of the oscillating tail. But the vortex rings generated by the sturgeon tail are oriented with an oblique axis and a central jet of fluid directed posteroventrally. This orientation indicates that the reaction force on the sturgeon is directed anterodorsally during steady horizontal locomotion, and suggests a new hypothesized force balance on swimming sturgeon. During steady horizontal locomotion at speeds less than 2 lengths/sec, sturgeon orient the body at an angle of between 8 and 25° to the flow (Wilga and Lauder, 1999). The reactive force from the vortex rings shed by the tail may be thus directed through the body near the center of mass.

The changing orientation of sturgeon tail triangles, the oscillatory pattern of the Y movement vector component, and the orientation of vortices shed behind the tail is not consistent with the classical hypothesis of heterocercal tail function for sturgeon. Furthermore, these data indicate that functional inferences based on the external shape of heterocercal tails may be erroneous. The dorsal lobe of the sturgeon tail does not lead during the tail beat, and the tail is extremely flexible. The similarity of heterocercal shape between the tails of the

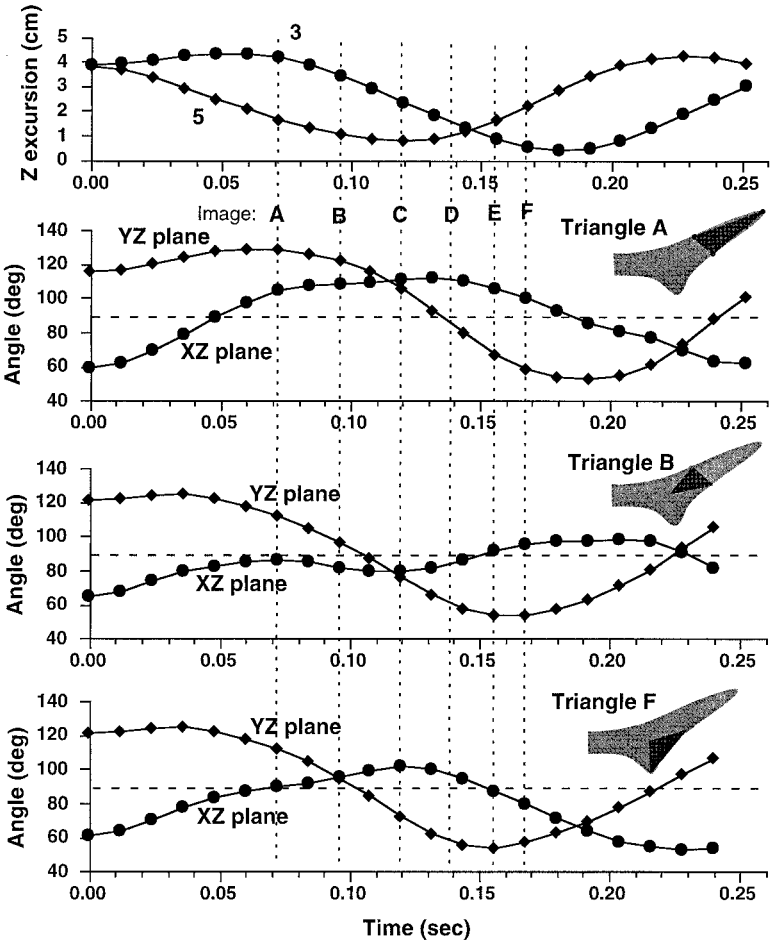

FIG. 9. Heterocercal tail kinematics in the sturgeon, *Acipenser transmontanus*. Z-dimension excursions (upper panel) of two points on the tail (see key to tail points in Fig. 10) and the three-dimensional angles of three tail triangles with the XZ and YZ planes. Letters A to F indicate the times corresponding to the similarly labeled video frames in Figure 8. Note the oscillation of the XZ angle about a value of 90° indicating that tail triangles are not maintaining a fixed orientation to the XZ plane.

leopard shark and sturgeon is not mirrored by similarity of function.

FUNCTION OF THE CAUDAL FIN DURING LOCOMOTION IN TELEOST FISHES

There is considerable diversity of tail shape within the teleost fishes. But given the near complete lack of three-dimensional kinematic data on the homocercal caudal fin of any teleost fish, bluegill sunfish (*Lepomis macrochirus*) were chosen for a detailed analysis of caudal fin function as a continuation of previous research on pectoral and dorsal fin kinematics in this centrarchid species (Gibb *et al.*, 1994; Jayne *et al.*, 1996; Lauder and Jayne, 1996).

Bluegill

Kinematics of the homocercal tail in bluegill were studied by swimming fish at 1.2, 1.6, and 2.2 lengths/sec in a flow tank as illustrated in Figure 5. Six markers were attached bilaterally to the tail (three each to the upper and lower lobes) to allow quantification of tail surface orientation in three-dimensions. Plots of marker Z-dimension excursions show that the dorsal lobe of the tail undergoes approximately a 50% greater

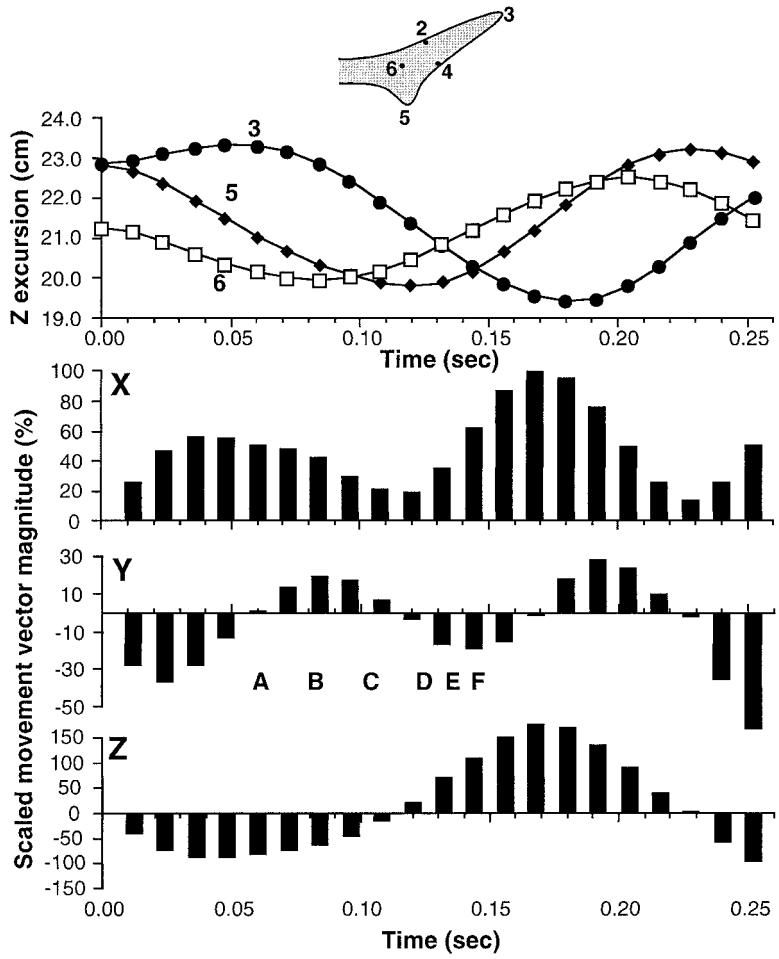

FIG. 10. Heterocercal tail kinematics in the sturgeon, *Acipenser transmontanus*. Z-dimension excursions (upper panel) of three points on the tail are shown for reference; the bottom three panels graph scaled movement vectors summed for all triangular elements on the tail in each of three-dimensions. Movement vectors were calculated according to the procedures described in Ferry and Lauder (1996) and reflect the projected area of the tail elements and the velocity of those elements (as components in each of three dimensions) for discrete time increments within the tail beat. Bar graphs have been scaled to 100% of maximum in the X-dimension. The higher the bar, the greater the velocity and area of the tail in that dimension. Positive X values reflect a vector pointing posteriorly, while a negative X-value would indicate a vector pointing anteriorly. Positive Y values indicate a vector pointing dorsally, while negative Y values reflect a vector oriented ventrally. Positive Z values indicate a vector pointing to the right and negative values a vector pointing to the left. Letters A to F in the Y panel indicate the times corresponding to the similarly labeled video frames in Figure 8. Note that as expected, positive thrust is developed throughout the tail beat as indicated by the consistently positive X values, and that the Z vector magnitudes alternate between left and right sides. However, the Y vectors unexpectedly show an alternation between negative and positive values which suggest that the tail is generating little net vertical force.

lateral movement than the ventral lobe (Fig. 11): the homocercal tail of bluegill thus functions asymmetrically during steady swimming. The relative movements of the dorsal and ventral markers did not change over the speed range of 1.2 to 2.2 lengths/sec. The tail increases in height during the tail beat, although this height increase is achieved by asymmetrical movements of the dorsal and ventral tail lobes. The ventral lobe expands within the first third of the tail beat while expansion of the dorsal lobe occurs in the final third (Fig. 11). The most dorsal marker also has a higher lateral ve-

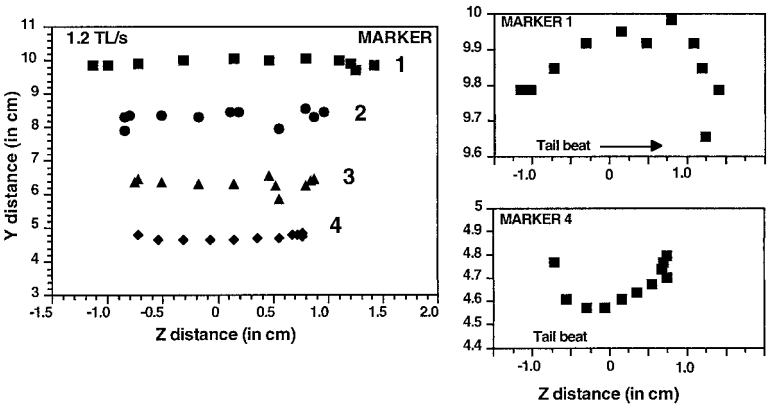

FIG. 11. Homocercal tail kinematics in a bluegill, *Lepomis macrochirus*, swimming at 1.2 lengths/sec. The positions of four markers on the trailing edge of the tail are shown in the YZ plane for one-half tail beat. Marker 1 is most dorsal while marker 4 is most ventral; the locations of these four markers on the tail are depicted in the video image of FIG. 5. Note that the dorsal marker undergoes a much greater excursion than the ventral marker. Movement of markers 1 and 4 is shown in more detail in the panels to the right. Note that the tail expands dorsoventrally (markers 1 and 4 move in opposite Y directions) and that the timing of this movement differs in the dorsal and ventral tail lobes indicating that the dorsal and ventral regions of the homocercal tail do not function similarly.

locity than the ventral (Table 1) at both 1.2 and 2.2 lengths/sec.

If the homocercal tail were functioning as a homogeneous flat vertical plate and generating a reactive force directly forward with no Y component (as the classical hypothesis predicts), the dorsal and ventral tail lobes should both maintain a 90° angle to the horizontal throughout the tail beat cycle. Measurement of projected YZ planar angles (Table 1; Fig. 12) shows that the dorsal lobe of the tail achieves a significantly acute angle to the horizontal while the ventral lobe is more vertically oriented but nonetheless still substantially acute. The homocercal bluegill tail is thus moving in a manner indicating that lift forces may be generated and that the reactive force on the body is not horizontal in orientation.

TABLE 1. *Movement of four markers (M1–M4, from dorsal to ventral) on the trailing edge of the caudal fin of bluegill sunfish (*Lepomis macrochirus*) during steady swimming at two speeds.**

Variable	1.2 lengths/sec	2.2 lengths/sec
M1 max Z velocity	24.7 cm/sec	46.4 cm/sec
M4 max Z velocity	17.2 cm/sec	40.6 cm/sec
M1–M2 min angle	67 deg.	69 deg.
M3–M4 min angle	77 deg.	75 deg.
M1–M4 phase lag	5.9%	7.3%

* Phase lags are in % tail beat cycle.

Calculation of three-dimensional planar angles confirms these changes in tail lobe orientation (Fig. 13). The dorsal lobe of the tail achieves an XZ planar angle of nearly 75°, significantly less than the 90° angle expected under the classical hypothesis of homocercal tail function. In addition, the minimum angle occurs just prior to midbeat when the tail passes the line of forward progression and velocity is highest.

What might be producing these asymmetrical tail movements? Is differential motion of the dorsal and ventral lobe possibly a passive consequence of internal skeletal asymmetries or is it actively generated? Most teleost fishes possess a complex set of intrinsic caudal fin muscles (Nursall, 1963; Nag, 1967; Cowan, 1969; Marshall, 1971; Winterbottom, 1974; Lauder, 1982, 1989) that have only rarely been studied experimentally. Anatomically, these muscles consist of dorsal and ventral flexor muscles (which often have deep and superficial components), the carinal muscles that connect the most dorsal and ventral skeletal elements of the tail to the dorsal and anal fins, and interradialis muscles (Fig. 14). These muscles are approximately symmetrically arranged about the horizontal axis and would seem to have generally symmetrical

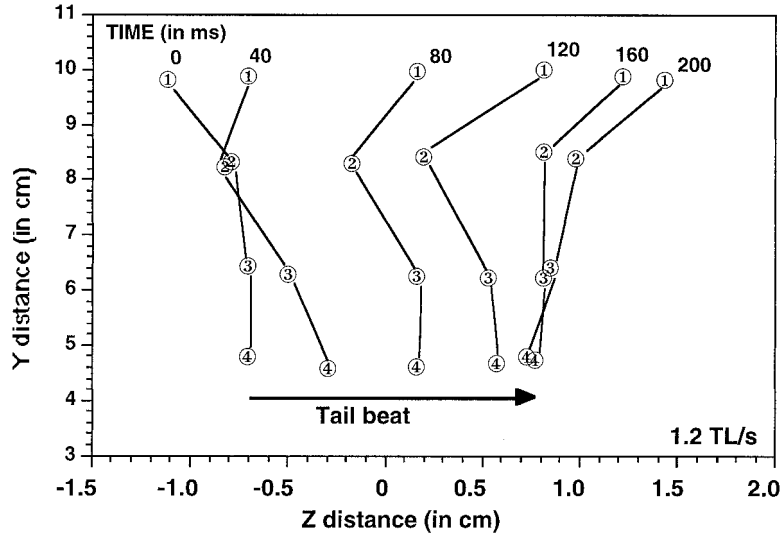

FIG. 12. Plot of the orientation of line segments in the YZ plane formed by posterior tail markers in bluegill swimming at 1.2 lengths/sec. Note that the dorsal tail lobe (segment 1–2) makes an acute angle to the horizontal as the tail beats from left to right. The ventral lobe (segment 3–4) changes orientation but remains more vertical than the dorsal lobe.

effects on dorsal and ventral tail lobes. But the hypochordal longitudinalis (HL) muscle possesses a fiber axis at an appreciable angle to the horizontal (Fig. 14: HL). The HL muscle originates from the ventrolateral surface of the caudal skeleton and passes posterodorsally to make four tendinous insertions on the first four fin rays. If the HL

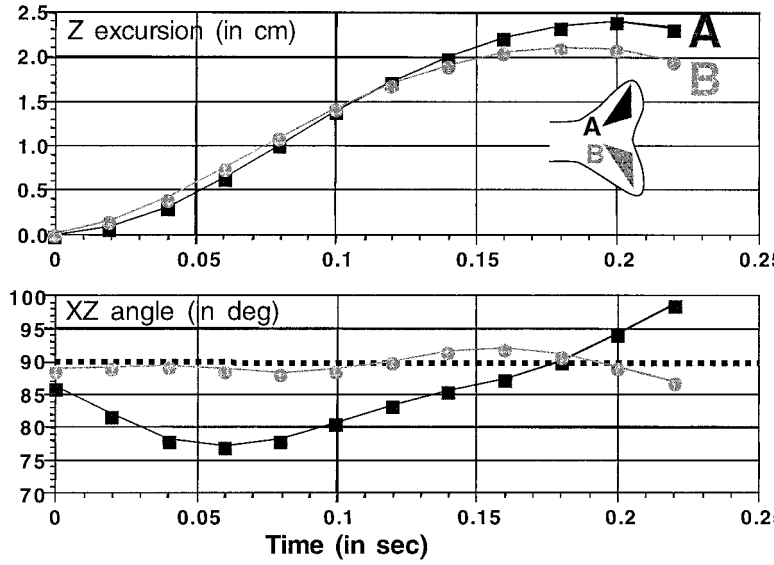

FIG. 13. Homocercal tail kinematics in bluegill, *Lepomis macrochirus.* Z-dimension excursions of the centroid of two triangular elements on the tail are shown for reference in the top panel. The three-dimensional angle of these two tail triangles with the XZ plane is plotted in the lower panel. Note that while the ventral lobe maintains a 3D angle near 90° during the tail beat, the dorsal lobe becomes significantly acute (less than 90°) indicating that dorsal lobe of the tail is moving at an angle predicted to generate lift forces.

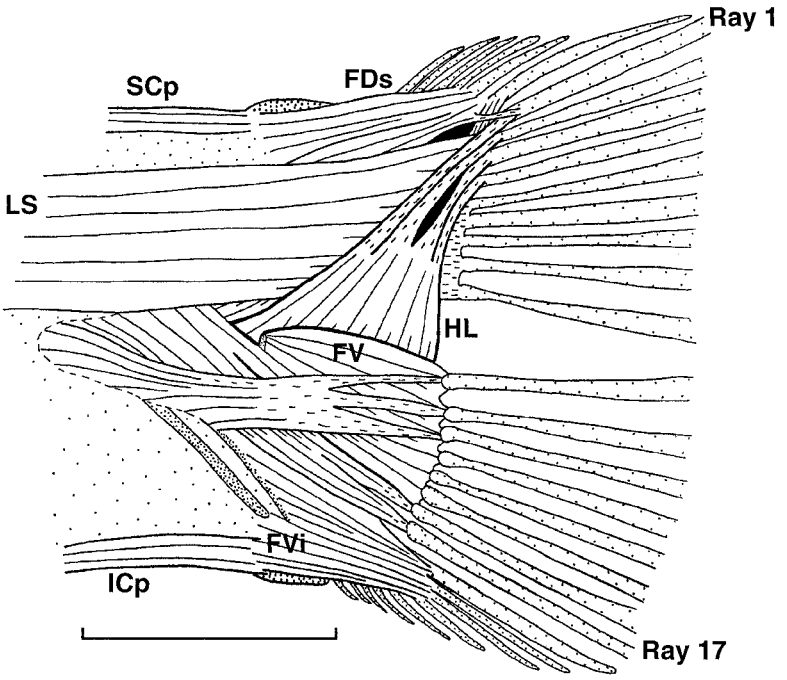

FIG. 14. Deep dissection of intrinsic caudal fin muscles in sunfishes, *Lepomis* (modified from Lauder, 1982). Note that the hypochordal longitudinalis muscle (HL) originates from the ventral region of the caudal skeleton and passes posterodorsally to insert tendinously on the first four fin rays. The HL is the only muscle in the tail with a fiber orientation at significant angle to the horizontal axis of the body. Superficial myotomal musculature and the interradialis muscles that interconnect fin rays have been removed. Scale bar is 1 cm. Abbreviations: FDs, flexor dorsalis superior; FV, flexor ventralis; FVi, flexor ventralis inferior; HL, hypochordal longitudinalis; Icp, infracarinalis posterior; LS, lateralis superficialis (myotomal muscle); SCp, supracarinalis posterior.

muscle is active during steady locomotion, it could cause the dorsal fin rays to lead the ventral rays during the tail beat, resulting in the kinematic pattern shown in Figures 11, 12, and 13.

Figure 15 shows that during slow steady swimming at 1.2 lengths/sec in bluegill, the HL muscle is indeed the only intrinsic caudal muscle that is active. Red fibers in myotomes of the caudal peduncle show light rhythmic bursting activity typical of locomotion at this speed, just above the transition from pectoral to caudal propulsion (Gibb *et al.,* 1994). The interradialis and flexor muscles within the tail show no activity at this speed. These data strongly support the hypothesis that asymmetrical function of the homocercal bluegill caudal fin is achieved actively as a result of intrinsic tail musculature.

What effect does this asymmetrical function of the dorsal and ventral tail lobes have on patterns of water flow in the wake? Quantitative flow visualization in the wake of bluegill swimming in a flow tank at 1.6 lengths/sec (Fig. 16) reveals regions of counterrotating vorticity which reflect a planar slice through a vortex ring in the wake. If the homocercal caudal fin is in fact generating a lift force as a consequence of asymmetrical motion of the dorsal and ventral tail lobes, then the vortex rings shed by the tail during horizontal swimming would be expected to generate a central jet of fluid with a slight ventral inclination to the horizontal. The flow pattern shown in Figure 16 reveals just such a pattern, and suggests a new hypothesis for the function of the homocercal tail in teleost fishes (Fig. 17).

The vortex wake produced by the tail of bluegill swimming horizontally is hypothesized to consist of a linked chain of rings each inclined ventrally so that the central jet of flow through the vortex core has a

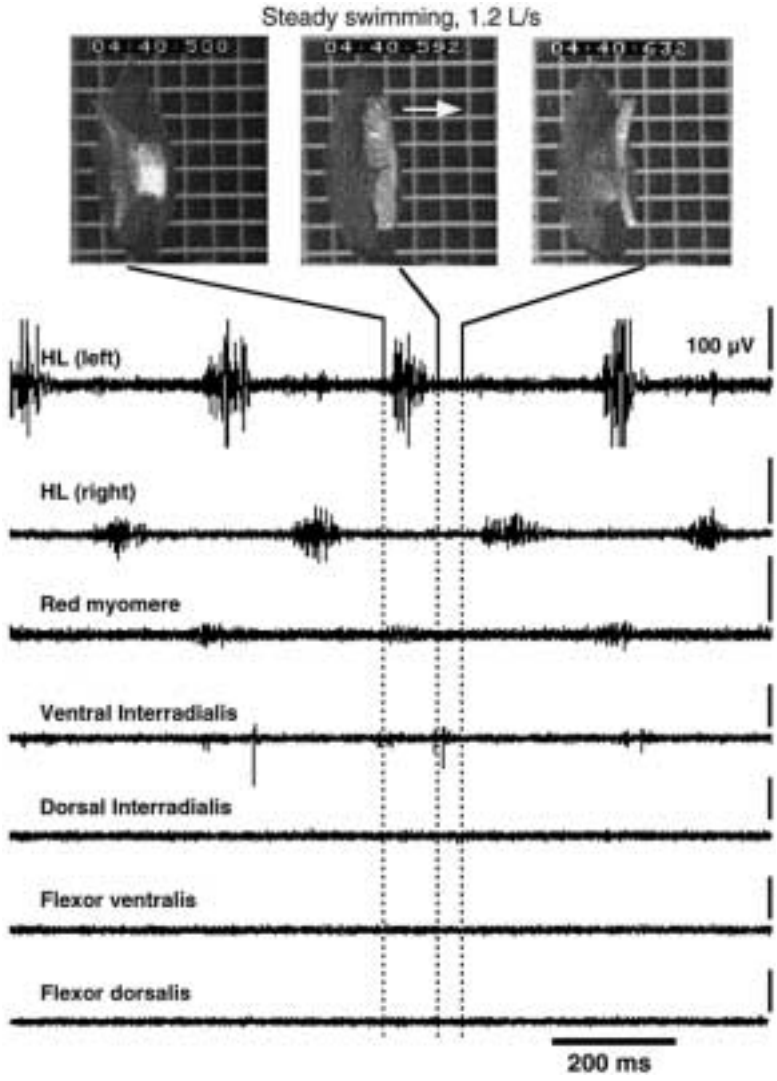

FIG. 15. Video frames (top, showing the posterior (YZ) view of tail motion) and electromyographic recordings (bottom) of intrinsic caudal muscles during steady swimming in bluegill (*Lepomis macrochirus*) at 1.2 lengths/sec. Note that at this speed, which is just above the transition from exclusively pectoral-based locomotion to caudal fin-based swimming, there is only slight activity in the myomeres in the caudal peduncle. The hypochordal longitudinalis muscle shows strong activity during steady swimming, but all other intrinsic tail muscles are inactive at this speed.

ventral (negative Y) component. The reactive force on the body produced by such a wake will have a dorsal (positive Y) component (Fig. 17) which will generate a torque about the center of mass. Such torques must be counteracted by lift forces generated by the head and/or pectoral fins anterior to the center of mass. Under this hypothesis, the homocercal tail functions in a similar manner to the classical model for the heterocercal tail: lift forces and torques are generated posteriorly.

Other teleosts

The asymmetrical function of the two lobes of the homocercal tail in bluegill might be considered an anomaly of lacustrine centrarchid fishes that is not shared by

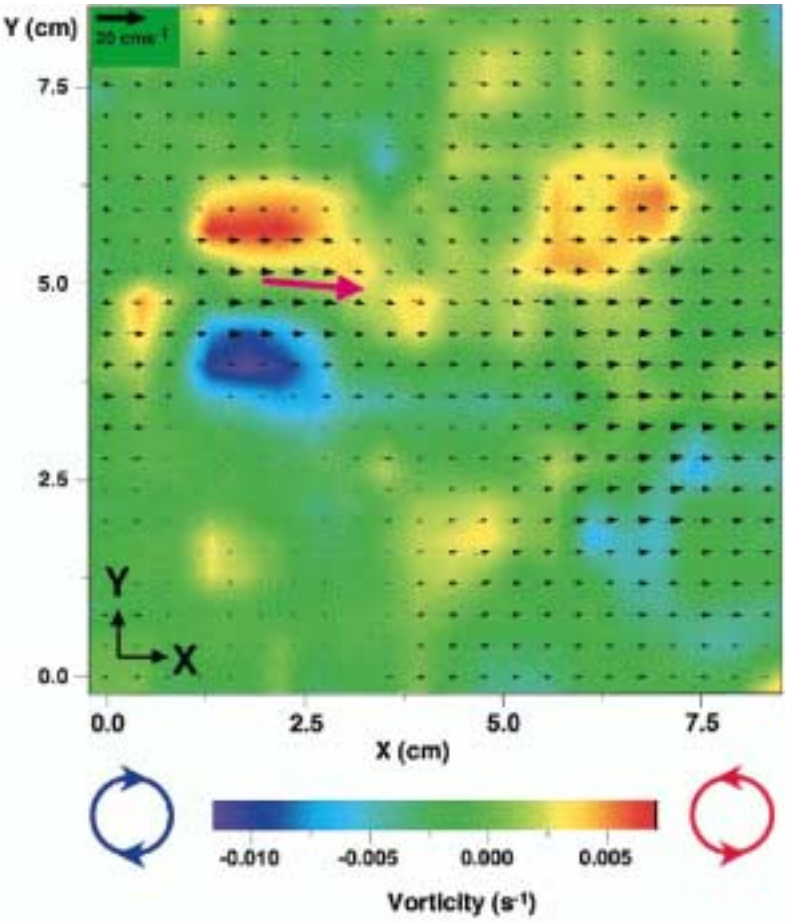

FIG. 16. Fluid velocity vectors (small arrows) and vorticity (colors) in a vertical plane behind the tail of a bluegill, *Lepomis macrochirus*, swimming at 1.6 lengths/sec. Vorticity was calculated using standard DPIV algorithms from the 20 × 20 matrix of velocity vectors. Mean flow velocity has been subtracted from the U (horizontal) component of the velocity vectors to better reveal changes in flow due to the tail beat; arrow in upper left gives the velocity vector scale. Reddish color indicates fluid rotation in a counter-clockwise direction, while blue colors reflects clockwise fluid rotation; green colors indicate minimal fluid rotation. Note that there are two prominent centers of counterrotating vorticity indicating that this plane has sliced a vortex ring. The central jet through the ring has a slight ventral inclination depicted diagrammatically by the large colored arrow.

other teleost fishes, particularly those that are capable of sustained high-speed locomotion. However, analysis of steady swimming in chub mackerel (*Scomber japonicus*) (Gibb *et al.*, 1999) reveals a similar pattern of asymmetry with the dorsal lobe undergoing a 15% greater Z excursion than the ventral lobe. The dorsal lobe also makes an angle of 80° to the XZ plane indicating that mackerel tails function in a similar general manner to bluegill and may generate lift even during steady horizontal swimming. Video images of the tail in eels (*Anguilla rostrata*) during swimming also show that the caudal fin undergoes complex patterns of deformation and does not function as a flat plate (Lauder and Gillis, in preparation).

Images or drawings of the tail of other teleosts swimming by Bainbridge (1963) and Aleev (1969) suggest that the homocercal tail of a diversity of teleost fishes exhibits asymmetry during horizontal locomotion. In addition, the hypochordal lon-

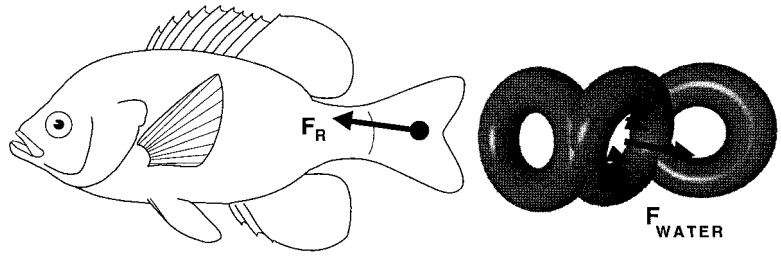

FIG. 17. Schematic illustration of the vortex wake behind a bluegill sunfish swimming steadily. Oscillatory motion of the tail is hypothesized to produce a linked chain of vortex rings (depicted for simplicity as circular and enlarged relative to tail height) which are tilted to form an acute angle to the XZ plane so that the central fluid jet through the ring has a posteroventral inclination. The outside diameter of vortex rings measured using DPIV closely approximates the height of the tail. The reactive force on the fish (F_R) is thus oriented anterodorsally. Under this hypothesis, the homocercal tail does not function in a manner consistent with the classical model, and generates lift forces and torques that must be balanced by anterior forces generated by the orientation and/or movement of the body and pectoral or pelvic fins.

gitudinalis muscle is found in virtually all teleost clades (Marshall, 1971; Lauder, 1989) and may be a key feature of the functional design of the teleost caudal fin. The functional patterns described above for bluegill are thus likely to be widespread among teleosts, although only a thorough comparative study of caudal function in fishes will reveal the extent of functional diversity.

SYNTHESIS

The experimental data described above on the function of heterocercal and homocercal and caudal fins suggests that a reevaluation of the classical models of both caudal fin types is needed. While the classical view of shark tail function was corroborated by the three-dimensional kinematic study of leopard sharks, the pattern of heterocercal tail function in sturgeon proved to be quite different. It is likely that further work will reveal considerable functional diversity among heterocercal tails. Based on experimental studies of heterocercal tails in two species, two different functional patterns have been observed. Hence, it is dangerous to speculate on general patterns of heterocercal tail function based solely on external morphology. Future quantitative studies of fluid flow over and in the wake of heterocercal tails are needed to refine functional hypotheses of heterocercal tail function, and analysis of flow over the body and pectoral fins will a more precise picture of the overall force balance.

These experimental data also indicate that the function of homocercal tails is considerably more complex than previously appreciated. External morphological symmetry is no guide to function: the symmetrical dorsal and ventral lobes of the homocercal tail may exhibit considerably different functional patterns with important consequences for the force balance on the body. The assumption of horizontal reaction forces based on morphological symmetry is certainly incorrect, as the homocercal tail is generating lift forces even during horizontal locomotion.

Finally, the significance of the diversity of tail designs in early vertebrates and major evolutionary patterns to tail morphology (Figs. 1, 2) is in need of reevaluation in the light of new functional data. Three-dimensional kinematic approaches and the ability to quantify fluid motion provide a previously unavailable perspective on the function of fish fins as control surfaces during swimming.

ACKNOWLEDGMENTS

Discussions with Alice Gibb, Gary Gillis, Cheryl Wilga, Eliot Drucker, Jimmy Liao, and Jen Nauen provided many insights in to fish locomotor dynamics and I am grateful to all of them. Jimmy Liao par-

ticipated jointly in the DPIV experiments on bluegill and sturgeon, and kinematic data on sturgeon were obtained in collaboration with Erin Schmidt. Previous work with Lara Ferry-Graham was critical in understanding the function of the shark tail. Collaborative research with Cheryl Wilga greatly increased my understanding of sturgeon locomotor function, and work with Alice Gibb and Kathy Dickson on mackerel tail function assisted in formulating my ideas on the function of homocercal tails. Heidi Doan assisted greatly with collection of kinematic data from bluegill. Thanks also to Corinne Connon, Jon Posner, and Derek Dunn-Rankin for their assistance in interpreting DPIV data on swimming fishes. Preparation of this manuscript was supported by NSF grant IBN 9807012 to GVL.

REFERENCES

Affleck, R. J. 1950. Some points in the function, development, and evolution of the tail in fishes. Proc. Zool. Soc. Lond. 120:349–368.

Aleev, Y. G. 1969. *Function and gross morphology in fish.* Translated from the Russian by M. Raveh. Keter Press, Jerusalem.

Alexander, R. M. 1965. The lift produced by the heterocercal tails of Selachii. J. Exp. Biol. 43:131–138.

Arratia, G. 1991. The caudal skeleton on Jurassic teleosts. A phylogenetic analysis. *In* M. M. Chang, Y. H. Liu, and G. R. Zhang (eds.), *Early vertebrates and related problems in evolutionary biology*, pp. 249–340. Science Press, Beijing.

Bainbridge, R. 1963. Caudal fin and body movements in the propulsion of some fish. J. Exp. Biol. 40: 23–56.

Bemis, W. E., E. K. Findeis, and L. Grande. 1997. An overview of Acipenseriformes. Env. Biol. Fish. 48:25–71.

Biewener, A. A. and R. J. Full. 1992. Force platform and kinematic analysis. *In* A. A. Biewener (ed.), *Biomechanics: Structures and systems,* pp. 45–73. Oxford University Press, Oxford.

Bone, Q. J. Kiceniuk, and D. R. Jones. 1978. On the role of the different fibre types in fish myotomes at intermediate swimming speeds. Fish. Bull. 76: 691–699.

Carroll, R. L. 1988. *Vertebrate paleontology and evolution.* W. H. Freeman and Co., San Francisco.

Carter, G. S. 1967. *Structure and habit in vertebrate evolution.* University of Washington Press, Seattle.

Cavagna, G. A. 1975. Force platforms as ergometers. J. Appl. Physiol. 39:174–179.

Cowan, G. I. 1969. The cephalic and caudal musculature of the sculpin *Myoxocephalus polyacanthocephalus* (Pisces: Cottidae). Can. J. Zool. 47:841–850.

Drucker, E. G. and G. V. Lauder. 1999. Locomotor forces on a swimming fish: Three-dimensional vortex wake dynamics quantified using digital particle image velocimetry. J. Exp. Biol. 202: 2393–2412.

DuBois, A. B., G. A. Cavagna, and R. S. Fox. 1976. Locomotion of bluefish. J. Exp. Zool. 195:223–35.

Ferry, L. A. and G. V. Lauder. 1996. Heterocercal tail function in leopard sharks: A three-dimensional kinematic analysis of two models. J. Exp. Biol. 199:2253–2268.

Fierstine, H. L. and V. Walters. 1968. Studies in locomotion and anatomy of scombroid fishes. Mem. South. Calif. Acad. Sci. 6:1–31.

Gibb, A. B., C. Jayne, and G. V. Lauder. 1994. Kinematics of pectoral fin locomotion in the bluegill sunfish *Lepomis macrochirus.* J. Exp. Biol. 189: 133–161.

Gibb, A., C. K. A. Dickson, and G. V. Lauder. 1999. Tail kinematics of the chub mackerel *Scomber japonicus*: Testing the homocercal tail model of fish propulsion. J. Exp. Biol. 202:2433–2447.

Gosline, W. A. 1971. *Functional morphology and classification of teleostean fishes.* University of Hawaii Press, Honolulu.

Grande, L. and W. E. Bemis. 1996. Interrelationships of Acipenseriformes, with comments on ''Chondrostei''. *In* M. Stiassny, L. Parenti and G. D. Johnson (eds.), *Interrelationships of fishes,* pp. 85–115. Academic Press, San Diego.

Gray, J. 1933. Studies in animal locomotion. I. The movement of fish with special reference to the eel. J. Exp. Biol. 10:88–104.

Gray, J. 1968. *Animal locomotion.* Weidenfeld and Nicolson, London.

Hebrank, M. R. 1982. Mechanical properties of fish backbones in lateral bending and in tension. J. Biomech. 15:85–89.

Helfman, G. S., B. B. Collette, and D. E. Facey. 1997. *The diversity of fishes.* Blackwell Science, Malden, Massachusetts.

Hildebrand, M. 1974. *Analysis of vertebrate structure.* John Wiley, New York.

Hopson, J. A. 1974. The functional significance of the hypocercal tail and lateral fin fold of anaspid ostracoderms. Fieldiana Geol. 33:83–93.

Jayne, B. C. and G. V. Lauder. 1994*a*. Comparative morphology of the myomeres and axial skeleton in four genera of centrarchid fishes. J. Morphol. 220:185–205.

Jayne, B. C. and G. V. Lauder. 1994*b*. How swimming fish use slow and fast muscle fibers: Implications for models of vertebrate muscle recruitment. Journal of Comparative Physiology A 175:123–131.

Jayne, B. C. and G. V. Lauder. 1995. Are muscle fibers within fish myotomes activated synchronously? Patterns of recruitment within deep myomeric musculature during swimming in largemouth bass. J. Exp. Biol. 198:805–815.

Jayne, B. C., A. Lozada, and G. V. Lauder. 1996. Function of the dorsal fin in bluegill sunfish: Motor patterns during four locomotor behaviors. J. Morphol. 228:307–326.

Johnsrude, C. L. and P. W. Webb. 1985. Mechanical properties of the myotomal musculo-skeletal system of rainbow trout, *Salmo gairdneri*. J. Exp. Biol. 119:71–83.

Johnston, I. A. 1991. Muscle action during locomotion: A comparative perspective. J. Exp. Biol. 160: 167–185.

Kardong, K. V. 1994. *Vertebrates. Comparative anatomy, function, evolution.* W. C. Brown, Dubuque.

Lauder, G. V. 1982. Structure and function of the caudal skeleton in the pumpkinseed sunfish, *Lepomis gibbosus*. J. Zool. Lond. 197:483–495.

Lauder, G. V. 1989. Caudal fin locomotion in ray-finned fishes: Historical and functional analyses. Amer. Zool. 29:85–102.

Lauder, G. V., C. Connon, and D. Dunn-Rankin. 1996. Visualization of flow behind the tail of swimming fish: New data using DPIV techniques. Amer. Zool. 36:7A.

Lauder, G. V. and B. C. Jayne. 1996. Pectoral fin locomotion in fishes: Testing drag-based models using three-dimensional kinematics. Amer. Zool. 36: 567–581.

Liao, J. and G. V. Lauder. 2000. Wake dynamics of the heterocercal tail in freely-swimming sturgeon (*Acipenser transmontanus*). Amer. Zool. 39:55A.

Lighthill, M. J. 1969. Hydromechanics of aquatic animal propulsion: A survey. Ann. Rev. Fluid Mech. 1:413–446.

Long, J. H. 1992. Stiffness and damping forces in the intervertebral joints of blue marlin (*Makaira nigricans*). J. Exp. Biol. 162:131–155.

Long, J. H. 1995. Morphology, mechanics, and locomotion: The relation between the notochord and swimming motions in sturgeon. Env. Biol. Fish. 44:199–211.

Magnuson, J. J. 1970. Hydrostatic equilibrium of Euthynnus affinis, a pelagic teleost without a gas bladder. Copeia 1970:56–85.

Marshall, N. B. 1971. *Explorations in the Life of Fishes.* Harvard University Press, Cambridge.

Moin, P. and J. Kim. 1997. Tackling turbulence with supercomputers. Sci. Am. 276:62–68.

Moy-Thomas, J. A. and R. S. Miles. 1971. *Palaeozoic fishes.* Saunders, Philadelphia.

Nag, A. 1967. Functional morphology of the caudal region of certain clupeiform and perciform fishes with reference to the taxonomy. J. Morphol. 123: 529–558.

Nakayama, Y. (ed.) 1988. *Visualized flow. Fluid motion in basic and engineering situations revealed by flow visualization.* Pergamon Press, Oxford.

Nieuwstadt, F. T. M. (ed.) 1993. *Flow visualization and image analysis.* Kluwer Academic Publishers, Dordrecht.

Nursall, J. R. 1963. The caudal musculature of *Hoplopagrus guntheri* Gill (Perciformes, Lutjanidae). Can. J. Zool. 41:865–880.

Patterson, C. 1968. The caudal skeleton in lower Liassic pholidophorid fishes. Bull. Br. Mus. Nat. Hist. Geol. 16:203–239.

Patterson, C. 1973. Interrelationships of holosteans. *In* P. H. Greenwood, R. S. Miles, and C. Patterson (eds.), *Interrelationships of fishes,* pp. 233–305. Academic Press, London.

Pough, F. H., J. B. Heiser and W. N. McFarland (eds.). 1989. *Vertebrate life, 3rd ed.* Macmillen, New York.

Raffel, M., C. Willert and J. Kompenhans. 1998. *Particle image velocimetry: A practical guide*. Springer-Verlag, Heidelberg.

Rayner, J. M. V. 1979. A new approach to animal flight mechanics. J. Exp. Biol. 80:17–54.

Rome, L. C., R. P. Funke, R. M. Alexander, G. Lutz, H. Aldridge, *et al.* 1988. Why animals have different muscle fibre types. Nature 335:824–827.

Rome, L. C., D. Swank and D. Corda. 1993. How fish power swimming. Science 261:340–343.

Romer, A. S. 1966. *Vertebrate paleontology.* University of Chicago Press, Chicago.

Schultze, H.-P. and G. Arratia. 1986. Reevaluation of the caudal skeleton of actinopterygian fishes. I. *Lepisosteus* and *Amia.* J. Morphol. 190:215–241.

Schultze, H.-P. and G. Arratia. 1988. Reevaluation of the caudal skeleton of actinopterygian fishes. II. *Hiodon, Elops* and *Albula.* J. Morphol. 195:257–303.

Shadwick, R., J. Steffensen, S. Katz, and T. Knower. 1998. Muscle dynamics in fish during steady swimming. Amer. Zool. 38:755–770.

Spedding, G. R. 1987. The wake of a kestrel (*Falco tinnunculus*) in gliding flight. J. Exp. Biol. 127: 45–57.

Spedding, G. R. and T. Maxworthy. 1986. The generation of circulation and lift in a rigid two-dimensional fling. J. Fluid Mech. 165:247–272.

Spedding, G. R., J. M. V. Rayner, and C. J. Pennycuick. 1984. Momentum and energy in the wake of a pigeon (*Columba livia*) in slow flight. J. Exp. Biol. 111:81–102.

Symmons, S. 1979. Notochordal and elastic components of the axial skeleton of fishes and their functions in locomotion. J. Zool. Lond. 189:157–206.

Thomson, K. S. 1971. The adaptation and evolution of early fishes. Quart. Rev. Biol. 46:139–166.

Thomson, K. S. 1976. On the heterocercal tail in sharks. Paleobiology 2:19–38.

Thomson, K. S. and D. E. Simanek. 1977. Body form and locomotion in sharks. Amer. Zool. 17:343–354.

Videler, J. J. 1975. On the interrelationships between morphology and movement in the tail of the cichlid fish *Tilapia nilotica* (L.). Neth. J. Zool. 25: 143–194.

Webb, P. W. and G. R. Smith. 1980. Function of the caudal fin in early fishes. Copeia 1980:559–562.

Westneat, M. W., W. Hoese, C. A. Pell, and S. A. Wainwright. 1993. The horizontal septum: Mechanisms of force transfer in locomotion of scombrid fishes (Scombridae, Perciformes). J. Morphol. 217:183–204.

Wilga, C. D. and G. V. Lauder. 1999. Locomotion in sturgeon: Function of the pectoral fins. J. Exp. Biol. 202:2413–2432.

Wilson, M. H. V. and M. W. Caldwell. 1993. New Silurian and Devonian fork-tailed ''thelodonts''

are jawless vertebrates with stomachs and deep bodies. Nature 361:442–444.
Winterbottom, R. 1974. A descriptive synonymy of the striated muscles of the Teleostei. Proc. Acad. Nat. Sci. Phil. 125:225–317.
Wolfgang, M. J., J. M. Anderson, M. Grosenbaugh, D. Yue, and M. Triantafyllou. 1999. Near-body flow dynamics in swimming fish. J. Exp. Biol. 202: 2303–2327.
Yang, W.-J. (ed.) 1989. *Handbook of flow visualization*. Hemisphere Publishing Corp., Washington.